Journal of the Atmospheric Sciences

Deep convection triggering by boundary layer thermals. Part 2: Stochastic triggering parametrization for the LMDZ GCM

--Manuscript Draft--

Manuscript Number:	
Full Title:	Deep convection triggering by boundary layer thermals. Part 2: Stochastic triggering parametrization for the LMDZ GCM
Article Type:	Article
Corresponding Author:	Nicolas Rochetin, Ph.D Columbia University New York, NY UNITED STATES
Corresponding Author's Institution:	Columbia University
First Author:	Nicolas Rochetin, Ph.D
Order of Authors:	Nicolas Rochetin, Ph.D
	Jean-Yves Grandpeix
	Catherine Rio
	Fleur Couvreux
Abstract:	This papers presents a stochastic triggering parametrization for deep convection and its implementation in the latest standard version of the LMD's GCM: LMDZ5b. The derivation of the formulation of this parametrization and the justification, based on LES results, for the main hypothesis was proposed in Part I of this study. Here the complete implementation and its link to the existing "Bulk" thermal plume model of Rio and Hourdin (2008) parametrization is presented. The parametrization is tested over various cases in a single column model (SCM) framework. An extensive sensitivity study to each introduced parameter is carried on. Eventually, the impact of the new triggering is then evaluated through the four precedent cases and in a 3D framework. It is found that the stochastic triggering (i) delays deep convection triggering over land, (ii) suppresses it over trade wind cumulus zones, and (iii) increases the day-to-day convective variability. The scale-aware nature of this parametrization is also discussed.
Suggested Reviewers:	Robert Plant r.s.plant@rdg.ac.uk
	George Craig George.Craig@dlr.de
	Anthony Del Genio anthony.d.delgenio@nasa.gov
	Leo Donner Leo.J.Donner@noaa.gov
	Jon Petch Jon.Petch@metoffice.gov.uk
	Robert Pincus robert.pincus@colorado.edu
	Anton Beljaars anton.beljaars@ecmwf.int

Page and Color Charge Estimate Form
Click here to download Page and Color Charge Estimate Form: Page_Charge_Estimation_Form_Part_2.pdf

Deep convection triggering by boundary layer thermals Part II : Stochastic triggering parametrization for the LMDZ GCM

Nicolas Rochetin *

Laboratoire de Météorologie Dynamique, Paris, France

Jean-Yves Grandpeix

Laboratoire de Météorologie Dynamique, Paris, France

Catherine Rio

Laboratoire de Météorologie Dynamique, Paris, France

Fleur Couvreux

CNRM-GAME, Météo-France and CNRS, Toulouse, France

* *Corresponding author address:* Nicolas Rochetin, Laboratoire de Météorologie Dynamique, Boite 99, 4, place Jussieu, F-75252 PARIS CEDEX 05, FRANCE

E-mail: nicolas.rochetin@lmd.jussieu.fr

ABSTRACT

This papers presents a stochastic triggering parametrization for deep convection and its implementation in the latest standard version of the LMD's GCM: LMDZ5b. The derivation of the formulation of this parametrization and the justification, based on LES results, for the main hypothesis was proposed in Part I of this study. Here the complete implementation and its link to the existing "Bulk" thermal plume model of Rio and Hourdin (2008) parametrization is presented. The parametrization is tested over various cases in a single column model (SCM) framework. An extensive sensitivity study to each introduced parameter is carried on. Eventually, the impact of the new triggering is then evaluated through the four precedent cases and in a 3D framework.

It is found that the stochastic triggering (i) delays deep convection triggering over land, (ii) suppresses it over trade wind cumulus zones, and (iii) increases the day-to-day convective variability. The scale-aware nature of this parametrization is also discussed.

1. Introduction

In the first paper of this series (Rochetin et al., 2012, hereafter Part I) a stochastic parametrization of deep convection triggering has been formally presented. It is based on a statistical analysis of cloudy thermal plumes in a Large Eddy Simulation (LES) of a moist convection case observed in Niamey (Niger) on July the 10th of 2006 during the AMMA (African Monsoon Multidisciplinary Analysis) campaign. First the PDFs (probability distribution functions) of the vertical velocities and of the plume cross-sections at cloud base were determined. Then, assuming that deep convection is due to plumes with sizes and maximum vertical velocities exceeding some thresholds, a probability of triggering could be determined. The triggering process could then be parametrized by using random numbers with uniform distribution between 0 and 1 and by triggering convection whenever the random number is smaller than the probability of triggering.

The present paper is devoted to an actual implementation of this parametrization in the AGCM (Atmospheric General Circulation Model) LMDZ5B and to the assessment of its performance in some case studies and in a global simulation.

In GCMs, such as LMDZ5B, where shallow and deep convection are represented by separate parametrizations, the triggering scheme is the part of the model that decides whether moist convection should be treated as shallow or deep. It acts at every time step, so that the triggering scheme decides when deep convection begins and when it ends. Over land it is thus an important driving process of the diurnal cycle of convection and of the frequency of occurence of deep convection.

This frequency is generally overestimated in GCMs (Bechtold et al. (2004)). In LMDZ5B simulations, for instance, convection triggers every day over Niamey during the monsoon season, in contradiction with observations where lapses of 2 or 3 days without rain are frequent. In addition, most of the current GCMs tend to predict a diurnal precipitation maximum around noon while satellite observations shows a precipitation maximum during mid-afternoon or evening over tropical land (Bechtold et al. (2004), Yang and Slingo (2001)). This shift of the simulated diurnal cycle is partly due to the triggering of deep convection occuring too early. Guichard et al. (2004) argue that this is partly correlated with the fact that convective parametrization do not represent the *"Transient regimes"* (Guichard et al. (2004)) between shallow and deep stages, in which convective boudary layer gradually deepens and produces significant clouds.

In the LMDZ5B general circulation model, deep convection occurrence and intensity are related to the lifting effect of sub-grid sub-cloud processes. This is done by introducing two quantities: the available lifting energy (ALE) and available lifting power (ALP) provided at the base of deep convective towers by sub-cloud processes (Grandpeix and Lafore (2010), Grandpeix et al. (2010)). This ALE/ALP system made it possible to simulate a reasonably good diurnal cycle of precipitation in a moist convection case study over land (Rio et al. (2009)). However the deep convection triggering still occured one hour too early.

The aim of this paper is to present the implementation in LMDZ5B of the triggering parametrization described in Part I and to verify that it does improve the behaviour of the model over land with respect to the two aforementioned deficiencies: (i) representing the transition phase from shallow to deep convection; (ii) simulating the variability of rain occurence in semi-arid regions such as Niamey (Niger). In LMDZ5B, the boundary layer thermals are represented by the thermal plume model of Rio and Hourdin (2008). However, the thermal plume scheme only provides informations about the plume height, total cloud cover and average velocity. Therefore the first step is to determine, thanks to the links established in Part I between cloud height and cloud-base cross-section, the variable describing the thermal plume field, i.e. average vertical velocity, average cloud-base cross-section and number of thermals in the grid cell. Once this is done, the triggering parametrization described in Part I may readily be used.

The paper is organized in 5 parts. The first part presents the model and the different cases investigated. The second part presents the parametrization design for the stochastic deep convection triggering. In the third part the parametrization is evaluated through the AMMA case study. In the fourth part a sensitivity study to the parameters is made. And finally the impact on the diurnal cycle of the new triggering parametrization is discussed.

2. Data and Methodology

a. The LMDZ Single Column Model

We rely on the Single Column Model (SCM) part of the General Circulation Model (GCM) LMDZ5b (Hourdin et al. (2012)) designed to perform climate change simulations for the 5th IPCC assessment report. The model has 39 levels in the vertical, with the grid stretched near-to-surface (first grid point at 35 m and 8 grid-points in the first kilometer) and a mean resolution of 800 m between 1-20 km, with 8 grid-points over 20 km (last point at 40 km). The Emanuel's cumulus parameterization (Emanuel (1991)) is used for moist convection. Its statistical parametrization of entrainment has been modified by Grandpeix et al. (2004) in order to improve the sensitivity of the simulated deep convection to tropospheric relative humidity. The Emanuel scheme computes also a total cloud water content coupled to a statistical cloud representation, which is based on the computation of a cloud fraction using a log-normal probability density function, as suggested by Bony and Emanuel (2001). No ice parameterization is present in that case.

Since the version used for the last IPCC report (2007), the SCM has been updated. The main improvement concerns the boundary layer and the deep convection parametrizations. Regarding the boundary layer, a new mass flux scheme (Rio and Hourdin (2008)) representing boundary layer thermals was introduced and combined with the diffusive-scheme proposed by Mellor and Yamada (1974). This scheme uses "bulk" plume approach and computes the following variables: the cumulus cloud top and base altitudes, the thermal plume vertical velocity profile, and the plume fractional coverage vertical profile. Regarding deep convection, a new formulation of deep convection triggering and closure has been recently implemented (see Hourdin et al. (2012) for details). The convection scheme is coupled to a parameterization of shallow moist convection induced by thermal plumes (Rio and Hourdin (2008)), and to a parameterization of wakes (cold pools) fed by unsaturated downdrafts (Grandpeix and Lafore (2010) and Grandpeix et al. (2010)). Each one of these parameterizations provides the deep convection scheme with an Available Lifting Energy (ALE) related to the convection triggering computation, and an Available Lifting Power (ALP) (see section 1) related to the convection closure computation (see Grandpeix and Lafore (2010) and Grandpeix et al. (2010)).

In LMDZ, the triggering energy is deterministic, and supposed equal to the maximum kinetic energy delivered by the sub-cloud layer processes such as the density currents ($\mathrm{ALE_{WK}}$) and the boundary layer thermals ($\mathrm{ALE_{BL}}$): $\mathrm{ALE} = \mathrm{Max}(\mathrm{ALE_{WK}}, \mathrm{ALE_{BL}})$. This kinetic energy is then compared with the CIN, such that the triggering criterion is $\mathrm{ALE} > |\mathrm{CIN}|$. Rio et al. (2009) showed that those modifications improved the diurnal cycle of precipitation over mid-latitude land.

The closure hypothesis suggested by Grandpeix and Lafore (2010) relates the cloud base mass-flux to the power resulting from subcloud processes:

$$M_b = \frac{\mathrm{ALP_{BL}} + \mathrm{ALP_{WK}}}{|\mathrm{CIN}| + 2w_b^2} \tag{1}$$

In which, (i) w_b is the vertical velocity at LFC, (ii) and $\mathrm{ALP} = \mathrm{ALP_{WK}} + \mathrm{ALP_{BL}}$ is the lifting power resulting from the cold pool mechanism (index $_{\mathrm{WK}}$, as wakes) and boundary layer processes (index $_{\mathrm{BL}}$). The thermal plumes contribution ($\mathrm{ALP_{BL}}$) is proportional to the 3rd order mean of the vertical velocity $\overline{w'^3}$ (see Rio et al. (2009) for more details), and the cold pool contribution ($\mathrm{ALP_{WK}}$) is proportional to the third order of the spreading velocity C^{*3}. A recent study conducted by Rio *et al.* 2012 stressed the importance of (w_{b}) in this particular coupling.

b. Triggering: the role of thermals and cold pools in LMDZ

1) Thermals

In the current LMDZ trigger parametrization, the deterministic plume model imposes a mean (Bulk) thermal inside the domain, whose maximum kinetic energy is taken from the maximum velocity along the plume:

$$\mathrm{ALE}_{\mathrm{BL,det}} = \frac{1}{2}\left(\max_z \left\{w'_{\mathrm{u}}(z)\right\}\right)^2 \tag{2}$$

2) Cold pools

Another subcloud process coupled to the deep convection is the cold pool mechanism. The cold pools are created by the rain re-evaporation in the clear air, their height closely corresponds to the cloud base. They ensure the deep convection maintenance along the afternoon through their available lifting energy $\mathrm{ALE}_{\mathrm{WK}}$. Their lifting energy depends on their kinetic energy, (given their spreading velocity C^*) which is supposed equal to their potential energy (WAPE, Wake Potential Energy) $\mathrm{WAPE} = -g\int_0^{h_w} \frac{\delta\theta_v}{\overline{\theta_v}} dz$. Where h_w is the wake height, $\delta\theta_v = \theta_{v,wake} - \theta_{v,ext}$ is the positive virtual potential temperature difference between the wake and its environment and (iv) $\overline{\theta_v}$ is the grid-scale averaged virtual potential temperature. Meaning that C^* is related to the square root of the potential energy stored by the cold pools $C^* = 2\sqrt{\mathrm{WAPE}}$.

In the model, especially over land surfaces, once deep convection has triggered, the cold pool mechanism largely dominates the boundary layer lifting processes both in terms of triggering ($\mathrm{ALE} \approx \mathrm{ALE}_{\mathrm{WK}}$) and closure ($\mathrm{ALP} \approx \mathrm{ALP}_{\mathrm{WK}}$) (not shown).

c. The 4 cases investigated

Four distinct cases studies are investigated through the SCM.

2 CASES OF AFTERNOON DEEP-CONVECTION TRIGGERING

- The AMMA (African Monsoon Multidsciplinary Analysis) case corresponds to a deep convection triggering case of an isolated thunderstorm over a semi-arid surface at mid-afternoon (around 15:40 LT), the 10th of July 2006 over Niamey (Niger). The atmospheric column of the SCM is forced by surface fluxes (latent and sensible) and by large scale convergence in accordance with the observations reported that day. The reader is referred to Lothon et al. (2011) and Couvreux et al. (2012) for more details.
- The EUROCS-DEEP case (EUROpean Cloud System) corresponds to an early-afternoon deep convection triggering case (around 13:00 LT) over the great plains of the Oklahoma state (USA), the 27th of June 1997. The SCM atmospheric column is forced by fluxes and large-scale advection.

2 CASES OF SHALLOW CONVECTION WITH NO TRIGGER

- The EUROCS-SHALLOW case is case of diurnal cycle of non precipitating cumulus clouds over the Oklahoma great plains, the 21th of June 1997. The SCM atmospheric column is forced by fluxes and large-scale advection.
- The BOMEX case (Barbados Oceanographic and Meteorological Experiment) is a trade-wind cumulus case in a quasi-steady regime over a tropical ocean, the 24th of June 1969. The SCM is forced by SST (Sea Surface Temperature), by large scale advection, and radiative tendancies are also prescribed.

3. The deep convection stochastic triggering parametrization

a. Reminder of Part I

Data from the LES (semi-arid) case AMMA were analyzed for the study of geometrical and dynamical properties of the cloudy thermal plumes at the LCL during the transition from shallow to deep convection. The plume cross-section spectrum is composed of two exponential distributions. The type-1 plumes concerns the smallest clouds that are not able to trigger deep convection. The type-2 plumes includes the largest structures that may turn into congestus or cumulonimbus. Only type-2 plumes are considered relevant for the coupling of the boundary layer with deep convection.

For this type of clouds, we propose in the first part a triggering formulation organized in three steps.

A preliminary condition is that the boundary layer must be cloudy to allow the deep convection triggering.

The first criterion governs the dynamical transition from a regime in which cumulus clouds cannot reach their level of free convection (LFC) (i.e stays under the inhibition layer (CIN)) to a transient regime where at least some cumulus overshoot the CIN but do not reach the high troposphere. The transition is dynamic; it takes place when the statistical maximum kinetic energy produced by the boundary layer thermal plumes at cloud base verifies:

$$\mathrm{ALE}_{\mathrm{BL,stat}} > |\mathrm{CIN}| \tag{3}$$

Where $\mathrm{ALE}_{\mathrm{BL,stat}}$ is:

$$\mathrm{ALE}_{\mathrm{BL,stat}} = \frac{1}{2}\mathcal{W}'^2_{\mathrm{max}} \tag{4}$$

In which $\mathcal{W}'_{\mathrm{max}}$ is the statistical maximum vertical velocity inside the largest plume of the domain:

$$\mathcal{W}'_{\mathrm{max}} = \overline{w'_{\mathrm{p}}}\left[1 + \sqrt{\ln\left(\frac{(\frac{S_2 \ln(N_2)}{\check{s}})^2}{2\pi}\right) - \ln\left(\ln\left(\frac{(\frac{S_2 \ln(N_2)}{\check{s}})^2}{2\pi}\right)\right)}\right] \tag{5}$$

Where (i) $\overline{w'_{\mathrm{p}}}$ is the domain averaged vertical velocity of the plumes at the cloud base, (ii) S_2 is the domain averaged cloud base cross-section corresponding to type-2 plumes, (iii) N_2 is the corresponding thermal plume population in the domain (area S_{d}), and (iv) $\check{s}$ is an arbitrary draft cross-section of reference (here it is 400 m^2). This dynamical criterion is based on a PDF approach in which type-2 plumes are supposed to follow an exponential distribution from which an estimated maximum cloud base cross-section $\mathcal{S}_{\mathrm{max}}$, and a corresponding maximum velocity $\mathcal{W}'^2_{\mathrm{max}}$ are extracted.

The second criterion governs the transition from the transient regime to the deep convection regime, in which, at least one of the overshooting cumulus of the domain reaches the high troposphere, becoming a congestus or a cumulonimbus cloud. Every timestep Δt, the no-trigger probability is:

$$\widehat{P}_{\Delta t} = \left[\left(1 - \exp(\frac{-S_{\mathrm{trig}}}{S_2})\right)^{N_2}\right]^{\frac{\Delta t}{\tau}} \tag{6}$$

Where, Δt is the timestep, S_{trig} is an arbitrary threshold cross-section and τ is an arbitrary decorrelation interval between two consecutive, independant cloud scenes (e.g 10 min). The probability that a random realisation S_{max} exceeds S_{trig} is equal to the probability that a random number $0 < \mathcal{R} < 1$ exceeds the no-trigger probability $\widehat{P}_{\Delta t}$. Hence, in a time period Δt, the stochastic triggering happens if:

$$\mathcal{R} > \widehat{P}_{\Delta t} \tag{7}$$

In order to merge those two thresholds, one may define the effective lifting energy $\mathrm{ALE_{BL,eff}}$ as follows:

$$\text{If } \mathcal{R} > \widehat{P}_{\Delta t} \text{ then } \mathrm{ALE_{BL,eff}} = \mathrm{ALE_{BL,stat}},\ \mathrm{ALE_{BL,eff}} = 0 \text{ otherwise} \tag{8}$$

As a result, the deep convection triggering criterion is:

$$\mathrm{ALE} > |\mathrm{CIN}| \text{ with } \mathrm{ALE} = \mathrm{Max}(\mathrm{ALE_{BL,eff}}, \mathrm{ALE_{WK}}) \tag{9}$$

Since the triggering criterion determines whether convection is active or not, it must be checked at every timestep, In the case that deep convection has already triggered, the procedure is the same, but with a decorrelation time $\tau' = 2\tau$ (supposing that the deep convective updraft's timescale is 2 times longer than the thermal plume updraft's one).

b. Thermal plume spectrum parametrization

In this subsection, the type-2 plume distribution parametrization is presented. This consists in retrieving from the actual LMDZ "bulk" thermal plume model (Rio and Hourdin (2008)) the plume spectrum characteristics (i.e N_2 and S_2). This parametrization considers an equivalence between the plume ensemble and a single thermal whose properties are equal to the domain averaged properties of the plume population. It provides an updraft velocity w'_{u} profile, a fractional coverage α_{tot} profile, a cumulus base altitude z_{lcl}, and a cumulus top altitude z_{top}. Some arbitrary hypothesis and some results from the LES analysis made in the Part I of this study are used for that.

1. The first hypothesis is that the unique deterministic thermal plume and the plume spectrum both cover the same surface S_{tot} in a given domain S_{d}:

$$N_1 S_1 + N_2 S_2 = S_{\mathrm{tot}} = \alpha_{\mathrm{tot}} S_{\mathrm{d}} \tag{10}$$

2. Second, since the ratio between the fractional coverage of the cloud population 1 and the whole cloud population varies from 20 to 30% all along the simulation, it is supposed constant for simplicity:

$$\frac{N_1 S_1}{\alpha_{\mathrm{tot}} S_{\mathrm{d}}} = \epsilon \tag{11}$$

3. The third hypothesis has already been discussed in Part I: it supposes that population 2 exhibits a linear relationship between the mean typical size of the cloud base $\sqrt{S_2}$, the mean cloud depth $\langle z_{\mathrm{top}} \rangle - \langle z_{\mathrm{lcl}} \rangle$ and the mean altitude of the Lifting Condensation Level $\langle z_{\mathrm{lcl}} \rangle$ over the plume population, giving the following quadratic formulation for S_2:

$$S_2 = \left[a(\langle z_{\mathrm{top}} \rangle - \langle z_{\mathrm{lcl}} \rangle) + b \langle z_{\mathrm{lcl}} \rangle \right]^2 \tag{12}$$

Once S_2 is determined, the combination of Eq 10 and Eq 11 gives:

$$N_2 = \frac{(1-\epsilon)\alpha_{\mathrm{tot}} S_{\mathrm{d}}}{S_2} \tag{13}$$

Therefore, Eq 12 and Eq 13 give a complete description of the plume population 2, with the 3 parameters $\{a : b : \epsilon\}$. In Part I, it has been shown that parameters $\{a = 1 : b = 0.3\}$ were consistent with the LES, for the AMMA case.

4. The last assumption is to identify the domain average plume velocity $\overline{w'_{\mathrm{p}}}$ with the single plume velocity w'_{u}, and to identify the arithmetic average of the LCL altitude $\langle z_{\mathrm{lcl}} \rangle$ with the single plume LCL altitude z_{lcl}, that is respectively:

$$\overline{w'_{\mathrm{p}}} = w'_{\mathrm{u}} \tag{14}$$

$$\langle z_{\mathrm{lcl}} \rangle = z_{\mathrm{lcl}} \tag{15}$$

Where (i) w'_{u} is the deterministic plume updraft velocity and (ii) z_{lcl} is the deterministic plume condensation level.

Concerning the average cloud top, since the thermal plume model cloud top z_{top} corresponds to the top of the highest thermal of the field, we cannot directly relate it to the arithmetic average $\langle z_{\mathrm{top}} \rangle$. Hence we have chosen to consider a coefficient α, such that:

$$\langle z_{\mathrm{top}} \rangle = z_{\mathrm{lcl}} + \alpha(z_{\mathrm{top}} - z_{\mathrm{lcl}}) \tag{16}$$

Where $\alpha = 0.33$ reveals a good accordance between LES and SCM (not shown).

c. *Sum up*

1) Algorithm

At this stage, the deep convection triggering algorithmn is entirely determined. At every timestep Δt:

i. A preliminary condition is to have cloudy plumes inside the domain.

ii. If the preliminary condition is verified, Eq 12, Eq 13 and parameters $\{a : b : \epsilon : \alpha\}$ give the type-2 plume spectrum characteristics, that is the pair $[N_2 : S_2]$

iii. Eq 14 combined with Eq 5 and introduced in Eq 4 gives the maximum kinetic energy $\mathrm{ALE}_{\mathrm{BL,stat}}$ yielded by the type-2 thermal at LCL. The first criterion (Eq 3) is tested.

iv. If the first criterion is verified, Eq 6 is computed and the resulting no-trigger probability $\widehat{P}_{\Delta t}$ is compared with a random sampe $\mathcal{R}$. The second criterion (Eq 7) is tested and Eq 8 gives the $\mathrm{ALE}_{\mathrm{BL,eff}}$ (the $\mathrm{ALE}_{\mathrm{BL,stat}}$ accounting for the deep convection triggering).

v. If the final test 9 is verified, then deep convection triggers and the decorrelation time becomes $\tau' = 2\tau$

2) Parameters

The parametrization comprises six parameters divided in two groups:

i. we name "plume parameters" the set of parameters relative to the parametrization of the plume spectrum, that is $\{a : b : \epsilon : \alpha\}$. These parameters are critical for computing S_2 and N_2, and are estimated here through the AMMA Case's LES data.

ii. we name "triggering parameters" the set of parameters relative to the triggering parametrization, that is $\{S_{\text{trig}} : \tau\}$ (the threshold cross-section S_{trig} and the decorrelation time τ). These parameters form a part of the no-trigger probability computation (Eq 6) and cannot *a priori* be estimated by any mean. Then, their estimation needs a sensitivity study carried out over various cases in order to draft a reasonable range of values.

3) Sensitivity to the domain area S_{D}

The domain area S_{d} considered influences N_2 through Eq 13. In a 3D model framework, S_{d} means the grid-cell area, but in a single column framework S_{d} has to be specified. Consequently, for each one of the case studies defined below, we must define an arbitrary reference area S_{d}.

For the AMMA case, the size of the domain is supposed equal to the LES performed by Couvreux et al. (2012) and similar to the field campaign area as well (see Lothon et al. (2011)): that is $S_{\text{d,Amma}} = 10^4$ km^2 (100 x 100 km). For the EUROCS DEEP and EUROCS SHALLOW cases, the arbitrary domain size is $S_{\text{d,Eu}} = 6,55.10^4$ km^2, consistently with the LES performed by Guichard et al. (2004) (which is in 2D with a domain lenght of 250 km). And for the BOMEX case, the domain size is supposed to be close to the field campaign area, which is $S_{\text{d,Bo}} = 2,5.10^5$ km^2 (500 x 500 km) according to Holland (1970). In the remaining of the paper, those reference areas will be held for each one of the case studies cited below.

4. Parametrization evaluation and estimation of the "plume parameters"

a. Model evaluation on the AMMA case

The SCM is run on the AMMA case, with a $\Delta t = 60$ s timestep, and the results are compared with LES (see Part I for the LES description). Fig 1 compares LES domain-averaged characteristics of the type-2 plumes with properties relative to the single plume parametrization (i.e given by the SCM) at the LCL. We shall notice first that, since deep convection only starts around 16:30 LT in the LES and gives rise to congestus and cumulonimbus clouds, which are not represented by the thermal plume model, the comparison between the LES and the SCM is not relevant from 16:30 LT to 18:00 LT.

Fig 1 a) shows that the SCM and the LES give similar velocities, and they both represent the afternoon velocity decrease, consistent with the sensible heat flux diminution (not shown). Then, since deep convection triggers in the mid-afternoon, it seems that the vertical velocity is not a correct proxi for describing the transition from shallow to deep convection.

Fig 1 b) compares the fractional coverage of the resolved vs parametrized thermal plumes at the LCL. The SCM looks consistent with the LES, even if SCM slightly overestimates the fractional coverage at cloud base, the time evolution of both looks quite similar, with an increasing trend from noon to mid-afternoon and a decreasing trend afterwards. This curve tends to show that the transition looks not well described by the fractional coverage, which does not exhibit a clear trend along the afternoon.

Fig 1 c) compares the cloud base and top of the resolved vs parametrized thermal plumes. As previously stated, the SCM starts to produce cumulus clouds later than the LES. The parametrized cumulus also have a lower cloud base and cloud top (by 200 to 400 m) and the cloud depth is overestimated from 15:00 onward, but the boundary layer deepening process is similarly represented in both simulations.

Those results suggest that the last hypothesis asserted for linking the thermal plume spectrum to the deterministic plume representation is, at least for the AMMA case, relevant. The deterministic parametrization of the boundary layer thermals is similar to the LES domain-averaged properties of the type-2 thermal plumes, and Eq 14, Eq 15 and Eq 16 seem relevant. Nevertheless, the thermal fractional coverage and the cloud depth are overestimated.

The next step is to constrain the thermal plume spectrum parametrization with the LES; that is to determine the so-called "plume parameters" $\{a : b : \epsilon : \alpha\}$.

Eq 12 with parameters $\{a = 1 : b = 0.3 : \epsilon = 0.3 : \alpha = 0.33\}$ are used in the SCM and the resulting S_2 and N_2 are compared with the LES in Fig 2 a) and b) respectively. The parametrized S_2 and N_2 are quite far from the LES from noon to about 15:00. The first reason is that the SCM starts to create cumulus later than the LES (see Fig 1). The other reason has already been discussed in the Part I (Fig 4) of this paper: when the first clouds appear inside the domain, the distinction between population 1 and 2 is not clear and the corresponding thermal plume cross-section distribution $\mathcal{P}(s)$ resembles more to a simple exponential than to a sum of exponential (see Part I Fig 4 a)). The population 2 distribution becomes more discernible later in the transition process, that is to say in that particular case, between 14:00 and 15:00 (see Part I Fig 4 a)). As a consequence, the couple $[S_2 : N_2]$ before mid-afternoon is highly correlated to the couple $[S_1 : N_1]$ (see errorbars in Part I Fig 4 c)). Therefore the only relevant values of S_2 and N_2 to be considered for the parametrization setting are in the 15:00-17:00 LT time range. And according to Fig 2, Eq 12 and Eq 13 with parameters $\{a = 1 : b = 0.3 : \epsilon = 0.3 : \alpha = 0.33\}$ give results in accordance with the LES (Fig 2) in this time range.

In the following, the set of constrained parameters hold for describing the cross-section spectrum (Eq 12 and Eq 13) is then

$\{a = 1 : b = 0.3 : \epsilon = 0.3 : \alpha = 0.33\}$.

b. Thermal plume spectrum characteristics over the 4 cases

1) Preliminary comments

This subsection is aimed at the study of the type-2 plumes cross-section spectrum over the 4 cases defined in Sec 2.3.

The deep convection scheme is removed there in order to examine the behaviour of the unperturbed thermal plume field during the transition. Indeed, after triggering, the precipitation and cold pools strongly modify the structure of the boundary layer. Here, our concern is the study of the thermal plume spectrum evolution with time, but still not the triggering.

The model is run with a timestep of $\Delta t = 450$s, that is, the timestep which is used in the actual standard version of LMDZ5B for climatological runs. That is the reason why the SCM exhibits oscillations, which were not present with a timestep of $\Delta t = 60$s. They result from numerical instabilities. Such instabilities can be suppressed with a much smaller timestep, but since the present parametrization is expected to be operational in a full GCM, it is important to test it in similar conditions as those required for long runs.

2) Spectrum characteristics

The simulated cloud base ($z_{\rm lcl}$) and cloud top ($z_{\rm top}$) altitude are plotted in Fig 3. Those value are given by the deterministic thermal plume model, thus, $z_{\rm lcl}$ and $z_{\rm top}$ express statistical mean values for the thermal plume pattern over an infinite domain. According to Fig 3, the parametrized boundary layer depth is sensitive to surface moisture; while increasing the surface dryness, the LCL altitude increases as well. Indeed, the semi-arid case AMMA exhibits the deepest boudary layer (around 2400 m) while the oceanic BOMEX case has the shallowest one (around 400 m). In the oceanic case BOMEX, there is no diurnal cycle of the cloud depth and cloud base altitude.

Table 1 displays the time evolution of the thermal plumes of category 2 characteristics, and Fig 4 shows their corresponding cloud base diameter ($d_2 = 2\sqrt{\frac{S_2}{\pi}}$) and spacing ($L_2 = \sqrt{1/D_2}$, where D_2 is spatial density $D_2 = \frac{N_2}{S_\mathrm{d}}$). Over continents (AMMA, EUROCS-DEEP and EUROCS SHALLOW), according to Eq 12, the average cross-section S_2 at the LCL increases during the transition phase, in association with the cloud deepening ($z_\mathrm{top} - z_\mathrm{lcl}$) and the cloud base elevation (z_lcl) given by the thermal plume model (see Fig 3). Inversely, accordingly to Eq 13, the total number of type-2 cumulus N_2 decreases, as well as their spatial density D_2. According to Eq 13, N_2 is inversely proportional to S_2. Hence, all along the transition, the boundary layer thermal structures become larger, deeper, and consequently less numerous in the domain considered. Fig 4 also shows that, along the continental transition phase the parametrization produces more spaced, as well as larger cloud structures: cloud centers starts from $L_2 = 3000$ m spacing at the beginning of the transition, and reach about $L_2 = 6000$ m at the end.

Eq 12 is at the core of this parametrization, and makes a direct link between the bulk plume and the spectral plumes, the parametrization is then very sensitive to both the cloud depth ($z_\mathrm{top} - z_\mathrm{lcl}$) and the cloud base altitude (z_lcl) simulated by the thermal plume model.

For the cases in which deep convection triggering has been observed (i.e AMMA and EUROCS DEEP), one can see that S_2 is two times more important in the AMMA case than EUROCS DEEP case at triggering. Indeed, even though clouds are deeper in the EUROCS DEEP case, the influence of z_lcl (the cloud base altitude) looks of primary importance over lands (in comparison with depth $z_\mathrm{top} - z_\mathrm{lcl}$) in controlling the horizontal cloud size.

Over ocean (BOMEX), cloud structures are more numerous, smaller and less spaced (see Table 1 and Fig 4), resulting in a spatial density D_2 often exceeding 1 cloud per km^2.

c. *Deterministic versus statistical ALE_{BL}*

Fig 5 displays $\mathrm{ALE}_\mathrm{BL,det}$ and $\mathrm{ALE}_\mathrm{BL,stat}$ (Eq 4) against CIN for all cases.

Let's focus first on continental cases. Depending on the case, $\mathrm{ALE}_{\mathrm{BL,stat}}$ exceeds $|\mathrm{CIN}|$ before of after $\mathrm{ALE}_{\mathrm{BL,det}}$. In the AMMA case the statistical $\mathrm{ALE}_{\mathrm{BL}}$ overcomes the inhibition around 13:15 LT, that is 1 hour after the deterministic one. But in the EUROCS DEEP case, the deterministic $\mathrm{ALE}_{\mathrm{BL}}$ crosses the inhibition 1 hours later than the statistical one (i.e around 11:15 LT). And both $\mathrm{ALE}_{\mathrm{BL}}$ triggers simultaneously (around 11:00) in the EUROCS SHALLOW case. Looking at those 3 continental cases, it is then difficult to extract a net effect of $\mathrm{ALE}_{\mathrm{BL,stat}}$ as compared with $\mathrm{ALE}_{\mathrm{BL,det}}$. This may even suggests that the deterministic is relevant for treating the continental cases

Looking at $\mathrm{ALE}_{\mathrm{BL,stat}}$ only, large differences can be seen whether the case in Fig 5. As shown in Eq 4, $\mathrm{ALE}_{\mathrm{BL,stat}}$ is mostly related to the thermal plume vertical velocity at the LCL w'_{u}, which both depends on the boundary layer buoyancy and boundary layer depth. In all the continental cases $\mathrm{ALE}_{\mathrm{BL,stat}}$ overcomes the CIN and a transient regime of several hours occurs during the afternoon, suggesting that strong updrafts feed overshooting cumulus. Regarding Fig 5, transition starts at 13:15 LT for the AMMA case, at 10:00 LT for the EUROCS DEEP case and at 11:00 LT for EUROCS SHALLOW case, which is quite consistent with LES. Concerning the EUROCS cases, the important $\mathrm{ALE}_{\mathrm{BL,stat}}$ in EUROCS SHALLOW is solely explained by the very large w'_{u} at LCL ($w'_{\mathrm{u}} \approx 2.2 \mathrm{m.s}^{-1}$).

In the oceanic case (i.e BOMEX), most prominent differences between $\mathrm{ALE}_{\mathrm{BL,det}}$ and $\mathrm{ALE}_{\mathrm{BL,stat}}$ appears. In this case $\mathrm{ALE}_{\mathrm{BL,stat}}$ stays most of the time below the CIN, but $\mathrm{ALE}_{\mathrm{BL,det}}$ is almost always superior to the $|\mathrm{CIN}|$. Indeed, the plume vertical velocity at LCL is two times lower in the BOMEX case ($w'_{\mathrm{u}} \approx 0.4$ $\mathrm{m.s}^{-1}$) than in the AMMA case ($w'_{\mathrm{u}} \approx 1$ $\mathrm{m.s}^{-1}$), resulting in a corresponding low value for $\mathcal{W}'_{\mathrm{max}}$ (see Eq 5). Therefore, the statistical $\mathrm{ALE}_{\mathrm{BL,stat}}$ cancels the deep convection triggering over an oceanic surface, in a subsiding atmosphere (e.g BOMEX). This aspect is of importance knowing that the standard version of the model constantly produces convective rain in excess in those regions.

d. An example of stochastic triggering in the AMMA Case

The SCM is run in the AMMA case, with the stochastic triggering for deep convection, with the plume parameters $\{a = 1 : b = 0.3 : \epsilon = 0.3 : \alpha = 0.33\}$ and the triggering parameters $\left\{S_{\mathrm{trig}} = 12\mathrm{km}^2 : \tau = 600\mathrm{s}\right\}$. Fig 6 exhibits the deep convection triggering scenario.

The thermal plume model does not create any cumulus (not shown) before 13:30 LT, explaining why $\mathrm{ALE}_{\mathrm{BL,stat}} = 0$. After 13:30 LT, some clouds appears and, a short time later the dynamical criterion is reached (Eq 3). The transient regime starts, meaning that at least one cloud hosts an updraft whose kinetic energy exceeds the CIN. A random generator is run and generates, every timestep, a random sample $\mathcal{R}$ (between 0 and 1) which is compared with a no-trigger probability $\widehat{P}_{\Delta t}$ calculated over the timestep period Δt. During the next hour the boundary layer and the surrounding clouds deepen (not shown), consequently, S_2 increases and N_2 decreases, which result in a slightly decrease of $\widehat{P}_{\Delta t}$. As long as the geometrical criterion is not verified (Eq 7), $\mathrm{ALE}_{\mathrm{BL,eff}} = 0$ deep convection cannot trigger (because Eq 9 is not verified). Around 14:30 LT a random realization $\mathcal{R}$ finally exceeds $\widehat{P}_{\Delta t}$; the geometrical threshold is reached (Eq 7) and deep convection triggers. A short time later the rain re-evaporation produces unsaturated downdraughts and cold pools, which ensures the deep convection triggering later on (not shown). The result is, for that particular run, a deep convection triggering delayed by around 1h15 as compared with the deterministic triggering, which triggers about 13:15 LT (not shown).

5. Sensitivity Experiments to the "triggering parameters" with the SCM

a. Integrated trigger probability $\mathcal{P}_{\Delta t}$

The main objective of this section is to explore the stochastic triggering sensitivity to the triggering parameters $\{S_{\mathrm{trig}} : \tau\}$ and the domain area S_{d}, in 4 distinct cases. The aim is to build, for every set of parameters, for each case, the diurnal cycle of the trigger probability.

A way to build it is to run a large number of simulations for every set of parameters and to retrieve the trigger histogram. But this is quite tedious and can be avoided. An alternative way is to run only one simulation for each case, in with the convection scheme switched off. Indeed, if deep convection triggering is cancelled the thermal plume model produces a unique, deterministic, time series of $[S_2 : N_2]$ pairs (Eq 12 and Eq 13). If we want to compute the probability that convection triggers on a time interval $[t_0,\ t_n]$ made of n timesteps of length Δt. We shall call this probability the integrated trigger probability $\mathcal{P}_{\Delta t}$. To that end, we first compute the no-trigger probability, which is the product of the no-trigger probabilities on each timestep:

$$\widehat{\mathcal{P}}_{\Delta t}(t_n) \ = \ \prod_{k=0}^{n-1} \widehat{P}_{\Delta t}(t_k)$$

Then the integrated trigger probability reads:

$$\mathcal{P}_{\Delta t}(t_n) = 1 - \prod_{k=0}^{n-1} \widehat{P}_{\Delta t}(t_k) \tag{17}$$

In that manner, we can deduce from a unique no-trigger scenario the time series of the integrated trigger probability $\mathcal{P}_{\Delta t}$ corresponding to a particular set of free parameters $\{S_{\text{trig}} : \tau\}$. Thus, the triggering sensitivity study requires only one convection-free simulation per case and per parameter configuration.

b. *Sensitivity to the threshold cross-section S_{trig}*

The first experiment concerns the triggering parameter S_{trig}, that is, the threshold (or critical) cloud base cross-section above which the cumulus cloud becomes a congestus (i.e deep convective cloud). The plume parameters are set to $\{a = 1 : b = 0.3 : \epsilon = 0.3 : \alpha = 0.33\}$, the decorrelation time is set to $\tau = 600$ s. For each case study, the domain area considered is the reference area (mentioned in Sec c).

Fig 7 displays the integrated trigger probability $\mathcal{P}_{\Delta t}$ for the range $S_{\rm trig} = \{10 : 12 : 15 : 18 : 20\}$ km^2 (i.e a critical diameter $D_{\rm trig} = \{3570 : 3910 : 4370 : 4790 : 5000\}$ m). The expected sigmoid shape occurs in several instances, but not always. Some curves display several steps or ramps (these peculiarities are commented below). The integrated trigger probability decreases when $S_{\rm trig}$ increases, in agreement with Eq 6 which shows that the no-trigger probability $\widehat{P}_{\Delta t}$ is an increasing function of $S_{\rm trig}$. For small values of $S_{\rm trig}$ the probability to trigger increases fast with cloud deepening $(z_{\rm top} - z_{\rm lcl})$ and cloud base elevation $(z_{\rm lcl})$. Hence, the triggering diurnal cycle is shifted earlier and more peaked (since, because cumulative probabilities are bounded by one, an increased probability to trigger early automatically makes it decrease later). While increasing $S_{\rm trig}$ the probabilistic triggering diurnal cycle is more spread along the afternoon, and the total probability $(\mathcal{P}_{\Delta t}(t_{\rm final}))$ is also reduced. For example the total trigger probability is 90% for $S_{\rm trig} = 18$ km^2 and 60% for $S_{\rm trig} = 20$ km^2 in the AMMA case, and even falls down to 12% for $S_{\rm trig} = 20$ km^2 in the EUROCS-Deep case.

One can notice that the EUROCS-Deep case exhibits, for intermediate values of $S_{\rm trig}$, a double peaked diurnal cycle of $\mathcal{P}_{\Delta t}$, with two distinct time periods favourable for triggering and a "suppressed" period in between. This can be understood by looking at Fig 3 (top right panel). Between 13:00 and 15:30 LT, the thermal plume model exhibits large oscillations, which lowers the cloud depth and increases the no-trigger probability to its maximum value $(\widehat{P}_{\Delta t} = 1)$.

The AMMA case looks also more favourable to triggering than the EUROCS DEEP case, even though both cases have a similar cloud depth. This is because the average cross-section (S_2) is an increasing function of the cloud base height (Eq 12).

The EUROCS SHALLOW case can trigger only for the smallest values of $S_{\rm trig}$ and, as mentioned earlier, the BOMEX simulation has no chance to trigger.

The first conclusion is that the altitude of the cloud base plays a key role for controlling the probabilistic triggering diurnal cycle in this parametrization, especially through Eq 12 and Eq 6. This parameter is actually the main discriminatory factor between those cases. Indeed, in all these cases the parametrized mean cloud depths are very close (around 600 m), but the integrated trigger probability increases with the cloud base height. Over wet soils or oceans, since the cloud base height is low, the cloud vertical extension must be more important than over dry surfaces to trigger deep convection, and the transition period is then longer. Indeed, even though overshooting cumulus are present (Eq 3) in the domain, their average cross-section S_2 is low because of a low z_{lcl} (Eq 12), and the no-trigger probability per unit time $\widehat{P}_{\Delta t}$ (Eq 6) stays very close to 1. Over dry soils clouds appears later, but since the boundary layer is deeper, thermal plumes structures and corresponding cloud bases are wider as well (following the hypothesis of a fixed aspect ratio for the boundary layer thermals). This results in a shorter transition period: the clouds needs less vertical extension to trigger deep convection. This can be verified when looking at Fig 5 and Fig 7 top panels; the AMMA transition period varies from 1h30 to more than 5h30 long (starting at 13:30), while the EUROCS Deep transition lasts from 2h30 to more than 7h30.

The second point is that an intermediate stage between shallow and deep regimes is now allowed. For instance, when $S_{\mathrm{trig}} = 20$ km^2, the total trigger probability for the AMMA Case is 70% while it is 10% for the EUROCS DEEP case. Thus, even though large scale and surface conditions still play a key role in the triggering (e.g cancels it in BOMEX), this new parametrization allows the model to have an "intermediate" stage, in which similar conditions can give different results. When increasing the threshold cross-section S_{trig}, this intermediate stage becomes more important.

c. *Sensitivity to the decorrelation interval τ*

The sensitivity of the probabilistic triggering diurnal cycle to the triggering decorrelation time τ is now approached. The chosen range of τ values (from 600 s to 900 s) is supposed to enclose the possible lifetimes of a boundary layer thermal feeding a cumulus cloud, and the threshold cross-section is set to $S_{\mathrm{trig}} = 12\ \mathrm{km}^2$.

From Eq 6, $\widehat{P}_{\Delta t}$ is an increasing function of τ. Indeed, an increase of the time period between two independent cloud scenes means a decrease by the same factor of the chance to trigger in a given period Δt. Actually, Fig 8 shows that an increase of τ reduces the integrated triggering probability (delaying so the triggering). This is more obvious in the EUROCS DEEP and the EUROCS SHALLOW cases than the AMMA case, because in the AMMA case all the triggering scenarios are concentrated in a very short period of time when $S_{\mathrm{trig}} = 12\ \mathrm{km}^2$ (i.e between 14:15 and 15:00 LT, see Fig 7 upper left panel).

d. Sensitivity to the domain area S_d

The model's sensitivity to the reference domain area S_{d} is now studied with paremeters $\left\{S_{\mathrm{trig}} = 12\mathrm{km}^2 : \tau = 600\mathrm{s}\right\}$.

Fig 9 shows that the parametrization reasonably reacts to a change in domain size S_{d}, favouring the triggering on larger domains. Indeed, the no-trigger probability per unit time $\widehat{P}_{\Delta t}$ (Eq 6) decreases with N_2: if considering a smaller (larger) domain, it is statistically more difficult (easy) to trigger deep convection. For all cases, the sensitivity to S_{d} resembles the sensitivity to S_{trig} but with the opposite sign; while increasing S_{d}, the triggering diurnal cycle shifts earlier and is more peaked. When multiplying by a factor $\beta = 10$ the surface domain of reference for the EUROCS-Shallow case, the probability to have triggered reaches 22% at the end of the simulation and 95% when $\beta = 100$. For the BOMEX case the triggering does not happen for the reason evoked earlier. To sum up; with this set of parameters, the model is almost sure to trigger deep convection within a day of simulation, over a land surface of 1000x1000 km.

This sensitivity to the domain size may be viewed like a "scale-dependant" parametrization, which favours triggering when coase resolutions are used. But thanks to the stochastic component it is not the case. Here, the stochastic component is essential for getting a "scale-aware" triggering parametrization, rather than a "scale-dependant" one. Indeed, if considering a particular domain, whatever the different ways to cut of this domain, the probability to trigger deep convection inside it remain unchanged when considering a large number of realizations.

6. Impact on the deep convection diurnal cycle and day-to-day variability

In this section the determinist and stochastic triggering with deep convection switched-on are compared. The model is now run with $\Delta t = 450$ s timestep. Each case is run with the deterministic triggering and the stochastic triggering with the "plume parameters" $\{a = 1 : b = 0.3 : \epsilon = 0.3 : \alpha = 0.33\}$, and the "triggering parameters" $\left\{S_{\mathrm{trig}} = 12\mathrm{km}^2 : \tau = 600\mathrm{s}\right\}$. The domain areas are taken as their reference value (defined in sec c).

a. Impact on the deep convection over land: AMMA and EUROCS-DEEP cases

In each one of these cases, two stochastic runs and a deterministic one are studied. The two stochastic runs correspond to different triggering scenarios, that is to different random samplings. The corresponding simulated diurnal cycles are compared in Fig 10 and Fig 11.

First, when comparing the deterministic triggering with the stochastic triggering, one can see that for both cases the stochastic parametrization significantly delays deep convection triggering (by 2 hours at least in both cases). Consequently, precipitation peak is delayed in a similar way. This is the direct consequence of adding a supplementary threshold (i.e a threshold cross-section) to the original dynamic threshold (i.e a threshold lifting energy) to enable triggering. As deep convection tends to inhibits boundary layer (turbulent diffusion and thermals) heating tendancies (see positive $Q_{1,\mathrm{BL}}$ in Fig 10 and Fig 11 right panels) through the sub cloud layer cooling induced by the convective rain re-evaporation (see negative $Q_{1,\mathrm{CV}}$ in Fig 10 and Fig 11 right panels), boundary layer mixing and deepening last longer in the stochastic case. The boundary layer low level heating (and drying) and low-tropospheric cooling (and moistening) effects continue later afternoon, giving a more continuous transition from the shallow to the deep regime as compared with the deterministic triggering (see Fig 10 and Fig 11 right panels). Indeed, the negative $Q_{1,\mathrm{BL}}$ zone (dashed contour in Fig 10 and Fig 11), which corresponds to the bulk cumulus simulated by the thermal plume model, clearly shows that the mean cumulus reaches a more developed stage before triggering in the stochastic run.

Then, the stochastic triggering allows a real transition period between shallow and deep regimes, this transition is not represented in the standard deterministic parametrization. This continuous transition is much more consistent with LES and observational data, at least for the AMMA (Lothon et al. (2011) and Couvreux et al. (2012)) and EUROCS-DEEP cases (Guichard et al. (2004)).

Looking now at the differences between the 2 stochastic triggering scenarios (Fig 10 and Fig 11 lower left panels), things are different depending on the case investigated. For the AMMA case, both stochastic runs trigger around 14:30 LT (Fig 10) (the fact that rainfalls only starts after 17:00 LT is caused by the convective adjustment time, which has been set to 8000 s in the model). Indeed, as shown in Fig 7 the integrated trigger probability (Eq 17) increases dramatically at that time, meaning that the time range for most of the triggering scenarios are concentrated in this short period of time. But for the EUROCS-DEEP case (Fig 11), the triggering scenarios differs from about 2 hours. Indeed, the trigger probability is more spread over the afternoon period (see Fig 7). Then, the stochastic component introduces *a priori* an intra day variability of the deep convection diurnal cycle.

Concerning the deep convetion intensity, in the AMMA case (Fig 10), both deterministic and stochastic runs exhibits similar diabatic heating rates $Q_{1,\mathrm{CV}}$. However, in the EUROCS-DEEP case (Fig 11) convection intensity is significantly weaker in the stochastic case. Actually, the fact that stochastically triggered deep convection uprises later has 2 contradictory effects. First, the triggering occurs in a deeper and drier boundary layer, and a moister low free troposphere (see Fig 12) because boundary layer processes last longer. The drier and deeper the boundary layer, the higher and colder the cold pools. Such developed cold pools shall *a priori* increase the cloud base mass flux through the ALP closure (see Eq 1), thus to have a stronger deep convection. But, when triggering later the CIN may also be higher (see Fig 5), and the present closure (Eq 1) should give a lower cloud base mass flux. In the AMMA case those effects look to compensate themselves, while in the EUROCS-DEEP case the second effect dominates.

b. Impact on the shallow convection: BOMEX and EUROCS-Shallow cases

According to the sensitivity study displayed in Fig 7, the deep convection has no chance to trigger in the BOMEX case and few chances in the EUROCS-SHALLOW case regarding the actual set of parameters. Therefore, in Fig 13 and 14, only one stochastic scenario (contrary to Fig 10 and 11) is considered and compared with the deterministic triggering.

One the one hand, the deterministic runs both trigger deep convection, and some precipitation are simulated in BOMEX. On the other hand, the stochastic runs do not trigger and $\mathrm{ALE}_{\mathrm{BL,eff}}$ is always 0.

In the BOMEX case, the absence of triggering is solely explained by the dynamic threshold (Eq 3). As already explained in Sec 4.3 (Fig 5) the statistical $\mathrm{ALE}_{\mathrm{BL,stat}}$ is below CIN, which cancels the deep convection triggering. In the EUROCS-SHALLOW case, both $\mathrm{ALE}_{\mathrm{BL,det}}$ and $\mathrm{ALE}_{\mathrm{BL,stat}}$ overcome the CIN approximately at the same time (around 11:30) but, in the stochastic run, the cloud depth and LCL altitude are not sufficient to produce suficiently large structures (S_2), and make significantly decrease the no-trigger probability ($\widehat{P}_{\Delta t}$,Eq 6). Indeed, $\widehat{P}_{\Delta t}$ stays very close to 1 (not shown) all along the day, forbidding so the triggering. Thus, in both stochastic runs, the boundary layer carries out 100% of the mixing processes and the cumulus cloud development is not altered by the counteracting effect of deep convection.

As already stressed in the previous subsection, this favours the presence of a drier boundary layer together with a moister lower free troposphere (not shown). But most of all, the present result opens the way to a better representation of the spatial, as well as temporal variability of the tropical moist convection. Indeed, the new parametrization make it possible to get an alternation, between dry and rainy days, as well as subsiding and ascending zones, and so could be an alternative to the long-standing bias of the LMDZ model to trigger almost everyday all over the Tropics.

c. Impact on the deep convection over a tropical ocean: the TOGA-COARE case

The COARE experiment (Coupled Ocean-Atmosphere Response Experiment) is part of the TOGA (Tropical Ocean-Global Atmosphere) campaign, conducted during the winter 1992-1993 over the western Pacific Warm-Pool. In the SCM, the corresponding run is 4-month long, and the prescribed SST and large scale forcing correspond to the field campagn observational data.

In the TOGA-COARE case, convective precipitation for the deterministic vs stochastic runs are very similar. The stochastic run allows deep convection triggering most of the time (as already noted in Sec 5.2). This is consistent with the fact that convective precipitations have been observed almost everyday of the observation period. In this case the important cloud depth acts to maintain a constantly low $\widehat{P}_{\Delta t}$ (not shown) through Eq 12 and Eq 6. Therefore, the stochastic triggering parametrization yields deep convection development over the thin but very moist boundary layer found over the Warm-Pool; the sensivity to the cloud depth is then critical in such situations.

d. *Impact on the 3D field: the day-to-day variability*

In order to assess the ability of the new trigger parametrization to perform reasonably well in a large range of conditions, we implemented it in the LMDZ5 GCM. The LMDZ model was run for 8 years with a resolution 96x95x39 and forced with climatological SSTs. No attempt was made to tune the model for a reasonable climate: results should be looked at from a purely qualitative point of view. Therefore, we won't pay attention to the precipitation rates, but only to the precipitation variability.

Fig 15 displays the convective precipitation time series simulated over a grid point located in the Sahel (nearly over Niamey) during the monsoon season. In both cases the large scale precipitation (i.e created by large-scale condensation processes) are negligible. However, the new trigger significantly increases the day-to-day variability of deep convection. Fig 15 shows that in the deterministic run, precipitation occurs almost everyday, while in the stochastic run it rains approximately every other day. This day-to-day variability is directly related to the introduction of a stochastic term in the triggering parametrization. Indeed, even if the large scale conditions are favourable, the new parametrization does not trigger unless a random number exceeds a certain value, yielding so a "stochastic variability". The consequence is that triggering is never "guaranteed", even if thermal plumes overcome CIN. This is of particular interest over such semi-arid zones - sometimes qualified "marginal zones" (Charney et al. (1977)), or "hot-spots" (Koster et al. (2004)) - in which the day-to-day variability is a major climatic component.

Then, those preliminary results suggest that the stochastic triggering parametrization drastically improves the model's representation of the day-to-day variability of deep convection in the Tropics. When switching back to the standard, deterministic triggering, the model tends to trigger everyday, which is a common bias shared by the majority of current GCMs.

7. Conclusions

The parametrization described in this paper derives from the analysis of LES data made in the Part I of this study. The study of the statistical properties of the thermal plume spectrum exhibited great advantages. It (i) first allowed to state hypotheses for building the thermal plume distribution parametrization, and (ii) suggested the existence of a supplementary, stochastic threshold governing the deep convection triggering. This resulted in a new formulation of the transition from shallow to deep convection, which includes a spectral representation of the cloudy thermal plumes, and a stochastic triggering of deep convection. From that, a stochastic parametrization of the deep convection triggering by boundary layer thermals has been proposed for the LMD's GCM (LMDZ5B). Among other considerations, we suppose a linear relationship between the mean cross-section of the plumes the LCL altitude and cloud depth extracted from the thermal plume model (developed by Rio and Hourdin (2008)). This parametrization includes so a computation of the thermal plume cross-section spectrum, and a computation of a no-trigger probability, whose exceedance by a random sampling determines whether triggering happens or not. It accounts for 6 parameters, among which three (a, b, ϵ and α) are related to the cloudy plumes spectrum computation (mean cross-section S_2 and population N_2), and the others (S_{trig} and τ) are related to the no-trigger probability computation ($\widehat{P}_{\Delta t}$).

A sensitivity study has been made over the threshold cross-section S_{trig} and the decorrelation time τ in order to explore some general features of the new stochastic triggering parametrization. (i) Over lands, the transition looks mostly governed by the cloud base altitude rather than the cloud depth. The higher LCL increases the cloud base size, which decreases the no-trigger probability, and favours so the deep convection triggering. Over drier surfaces, the transient regime between shallow and deep convection is then shorter. (ii) Over oceans or wet surfaces, since the cloud base is relatively low, the parametrization suggests a longer transition, which is mostly governed by the cloud depth. (iii) The parametrization is scale-aware, that is sensitive to the domain area considered, but insensitive to the domain cut-out. Actually, given the large scale conditions, the Monte Carlo process statistically conserves the same probability to trigger in a given domain, whatever the number of grids. (iv) The triggering is still ruled in a great part by the large scale and the surface conditions, but allows the presence of an intermediate stage between the shallow and the deep regime, in which stochastic processes can deeply affect the diurnal cycle scenario. The triggering appears like a scarse process, which has a certain probability to occur given the large scale and the surface conditions; meaning that even in favourable conditions deep convection may not trigger, as well as it can trigger in an unfavourable environment.

Then, the new parametrization has been tested over various academic cases in a single column framework and compared with the deterministic one. First, the new computation of $\mathrm{ALE}_{\mathrm{BL}}$ and the introduction of a geometric threshold (S_{trig}) act, respectively, to cancel deep convection over trade wind cumulus zones, and to delay it over land. This results in a longer transition period between the shallow and the deep regimes, in which cumulus clouds continue to grow and boundary layer continues to deepen later on. Second, the stochastic component give rises to an intra-day and a day-to-day variability, which is not present in the deterministic triggering. The 3D climatologic run confirms the presence of a day-to-day variability of convection. Therefore, the stochastic triggering may open the way to both improve the GCM's representation of the transition between shallow and deep stages, as well as the intra day and day-to-day variability of convection, which are poorly represented in most of current GCMs.

8. Figures and tables

a. Figures

b. Tables

Acknowledgments.

The research leading to these resulthas been both supported by the French Department of Teaching and Research, and by the European Union, Seventh Framework Program (FP7/2011-2015) under grant agreement n 282672. The author would like to thank Franoise Guichard and Jean-Philippe Lafore, from Meteo-France (Toulouse), for their very helpful comments, and for the numerous and enlightening discussions we had about deep convection issues.

REFERENCES

Bechtold, P., J. Chaboureau, A. Beljaars, A. Betts, M. Köhler, M. Miller, and J. Redelsperger, 2004: The simulation of the diurnal cycle of convective precipitation over land in a global model. *Quarterly Journal of the Royal Meteorological Society*, **130 (604)**, 3119–3137.

Bony, S. and K. Emanuel, 2001: A parameterization of the cloudiness associated with cumulus convection; evaluation using toga coare data. *Journal of the Atmospheric Sciences*, **58 (21)**, 3158–3183.

Charney, J., W. Quirk, S. Chow, and J. Kornfield, 1977: A comparative study of the effects of albedo change on drought in semi-arid regions. *Journal of the Atmospheric Sciences*, **34 (9)**, 1366–1385.

Couvreux, F., C. Rio, F. Guichard, M. Lothon, G. Canut, D. Bouniol, and A. Gounou, 2012: Initiation of daytime local convection in a semi-arid region analysed with high-resolution simulations and amma observations. *Quarterly Journal of the Royal Meteorological Society*, **138 (4)**, 56–71.

Emanuel, K., 1991: A scheme for representing cumulus convection in large-scale models. *Journal of the atmospheric sciences*, **48 (21)**, 2313–2335.

Grandpeix, J. and J. Lafore, 2010: A density current parameterization coupled with emanuel's convection scheme. part i: The models. *Journal of the Atmospheric Sciences*, **67 (4)**, 881–897.

Grandpeix, J., J. Lafore, and F. Cheruy, 2010: A density current parameterization coupled with emanuel's convection scheme. part ii: 1d simulations. *Journal of the Atmospheric Sciences*, **67 (4)**, 898–922.

Grandpeix, J., V. Phillips, and R. Tailleux, 2004: Improved mixing representation in emanuel's convection scheme. *Quarterly Journal of the Royal Meteorological Society*, **130 (604)**, 3207–3222.

Guichard, F., et al., 2004: Modelling the diurnal cycle of deep precipitating convection over land with cloud-resolving models and single-column models. *Quarterly Journal of the Royal Meteorological Society*, **130 (604)**, 3139–3172.

Holland, J., 1970: Preliminary report on the bomex sea–air interaction program. *Bull. Amer. Meteor. Soc*, **51 (9)**, 815–816.

Hourdin, F., et al., 2012: Lmdz5b: the atmospheric component of the ipsl climate model with revisited parameterizations for clouds and convection. *Climate Dynamics, in Press*, 1–30.

Koster, R., et al., 2004: Regions of strong coupling between soil moisture and precipitation. *Science*, **305 (5687)**, 1138–1140.

Lothon, M., B. Campistron, M. Chong, F. Couvreux, F. Guichard, C. Rio, and E. Williams, 2011: Life cycle of a mesoscale circular gust front observed by a c-band doppler radar in west africa. *Monthly Weather Review*, **139**, 1370–1388.

Mellor, G. and T. Yamada, 1974: A hierarchy of turbulence closure models for planetary boundary layers. *Journal of the Atmospheric Sciences*, **31 (7)**, 1791–1806.

Rio, C. and F. Hourdin, 2008: A thermal plume model for the convective boundary layer: Representation of cumulus clouds. *Journal of the atmospheric sciences*, **65 (2)**, 407–425.

Rio, C., F. Hourdin, J. Grandpeix, and J. Lafore, 2009: Shifting the diurnal cycle of parameterized deep convection over land. *Geophys. Res. Lett*, **36**, L07 809.

Yang, G. and J. Slingo, 2001: The diurnal cycle in the tropics. *Monthly Weather Review*, **129 (4)**, 784–801.

List of Tables

	AMMA			EUROCS DEEP			BOMEX			EUROCS SHALLOW		
Local time	S_2	N_2	D_2	S_2	N_2	D_2	S_2	N_2	D_2	S_2	N_2	D_2
8	0	0	0	0	0	0	0.34	76406	0.306	0	0	0
9	0	0	0	0	0	0	0.29	348299	1.393	0	0	0
10	0	0	0	0	0	0	0	0	0	0.16	18346	0.280
11	0	0	0	0.53	15325	0.234	0.27	277350	1.109	0.64	3750	0.057
12	0	0	0	0.8	8667	0.132	0.25	325149	1.301	0.71	3100	0.047
13	0	0	0	1.14	5136	0.078	0.17	653996	2.616	0.79	2278	0.034
14	0.65	1842	0.184	1.14	5934	0.091	0.24	332943	1.331	0.88	1743	0.027
15	2.16	513	0.051	1.56	4099	0.063	0.33	213492	0.854	0.87	1586	0.024
16	2.15	332	0.033	1.56	3901	0.060	0.36	322005	1.288	0.87	1550	0.024
17	2.15	304	0.030	1.56	3001	0.046	0.36	323064	1.292	0.87	1699	0.026
18	2.15	265	0.027	0	0	0	0.27	170473	0.682	0	0	0

TABLE 1. Type-2 plume spectrum characteristics time evolution simulated by the SCM with deep convection switched off: mean cross-section S_2 (km^2), population N_2, and spatial density D_2 (km^{-2})

List of Figures

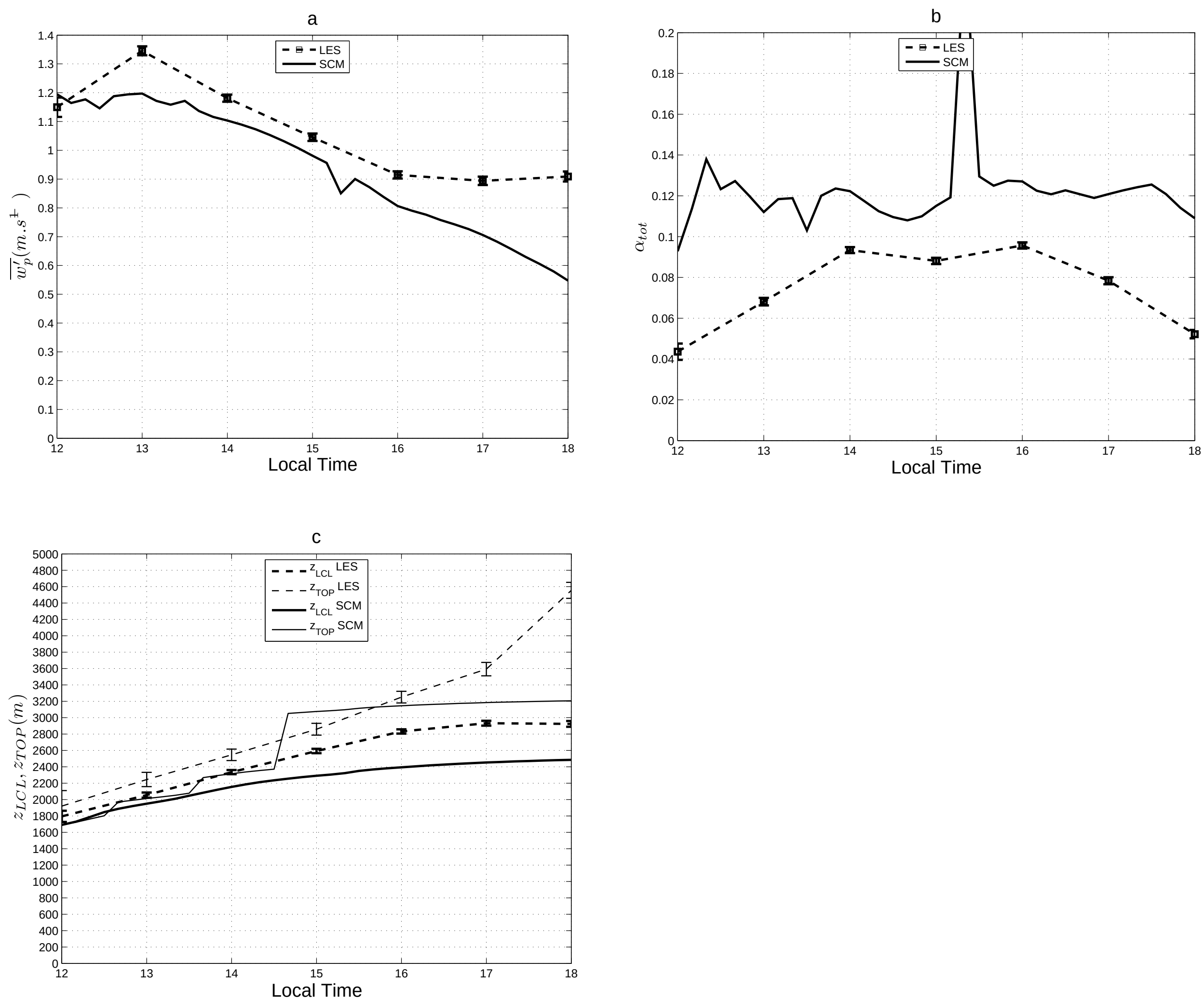

FIG. 1. AMMA Case, characteristics of the plume field at the LCL: a) Mean vertical velocity over the plume field $\left\langle \overline{w'_{\mathrm{p}}} \right\rangle$ (m.s^{-1}, see Eq 16 with $\alpha = 0.33$) computed from the LES (dashed) against single plume velocity w'_{u} simulated by the SCM (solid) with deep convection switched off, b) Same for the fractional coverage α_{tot}, c) Same for cloud base (thick) and cloud top (thin)

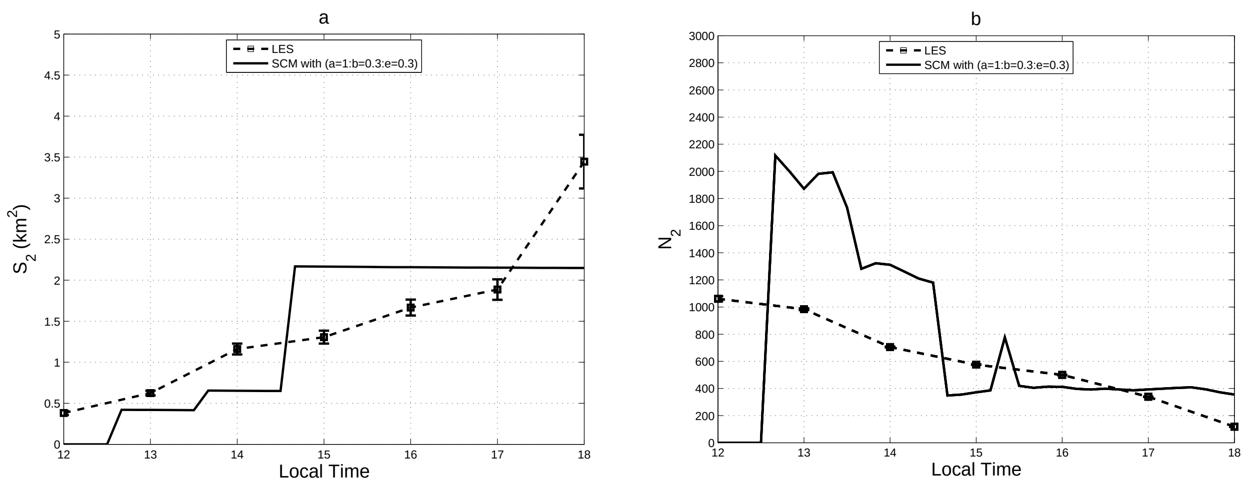

FIG. 2. AMMA Case: Time evolution of (a) the mean cross-section area of thermals 2 S_2 (km^2), (b) the thermals 2 population N_2 from LES (dashed) and SCM simulation (solid) with deep convection switched off

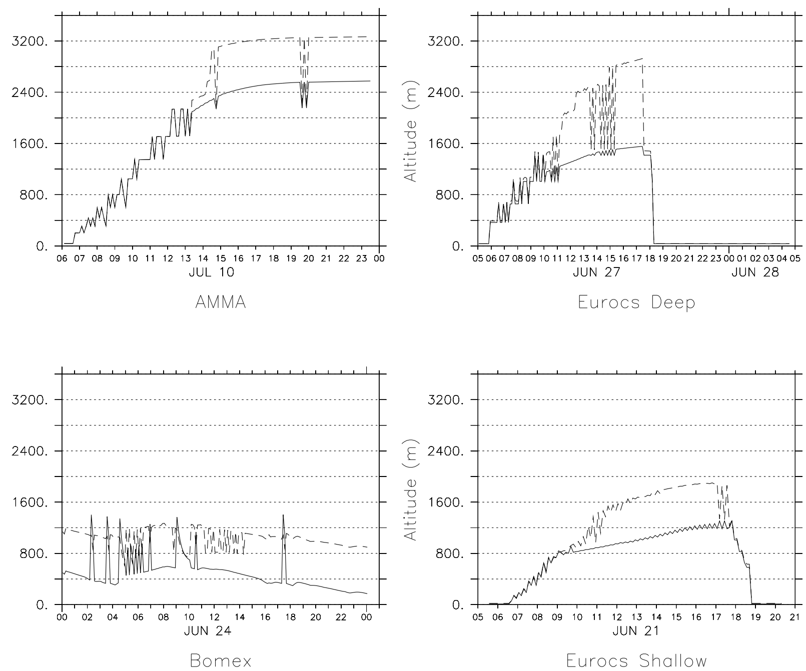

FIG. 3. Cloud base z_{lcl} (solid) and cloud top z_{top} (dashed) altitudes (m) extracted from the SCM for the cases AMMA, EUROCS Deep, BOMEX and EUROCS Shallow simulated by the SCM with deep convection switched off

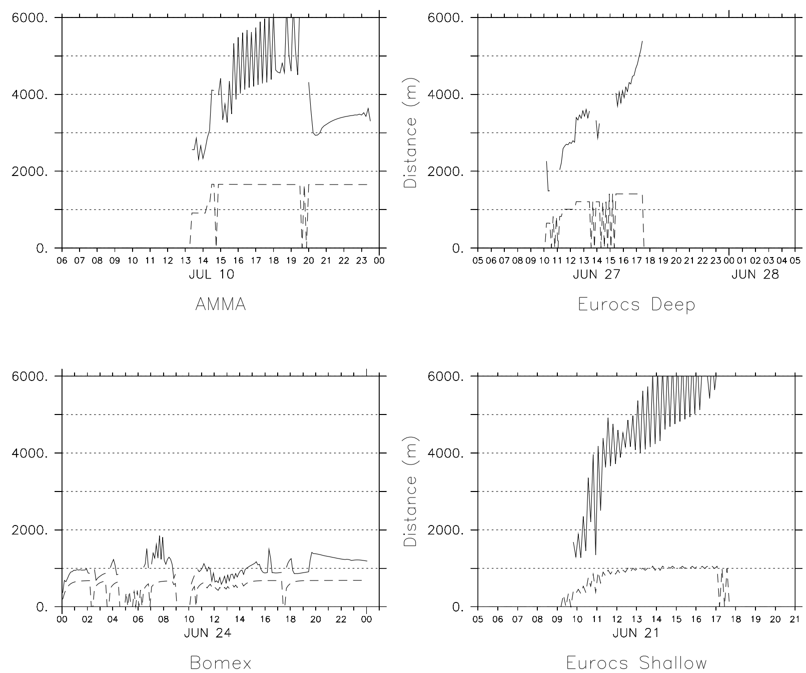

FIG. 4. Mean cloud base diameter d_2 (m) (dashed) and spacing L_2 (m) (solid) of thermal plumes of category 2 simulated by the SCM with deep convection switched off. The plume parameters are $\{a = 1 : b = 0.3 : \epsilon = 0.3 : \alpha = 0.33\}$

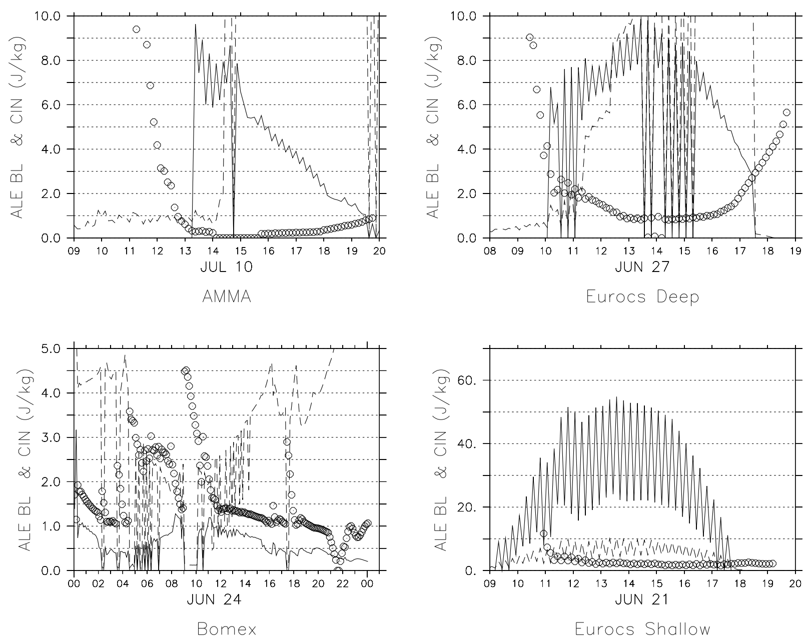

FIG. 5. Statistical Available Lifting Energy $ALE_{BL,stat}$ (solid, $m^2.s^{-2}$), deterministic $ALE_{BL,det}$ (dashed), and CIN (circles, $J.kg^{-1}$) simulated by the SCM with deep convection switched off. The plume parameters are $\{a = 1 : b = 0.3 : \epsilon = 0.3 : \alpha = 0.33\}$

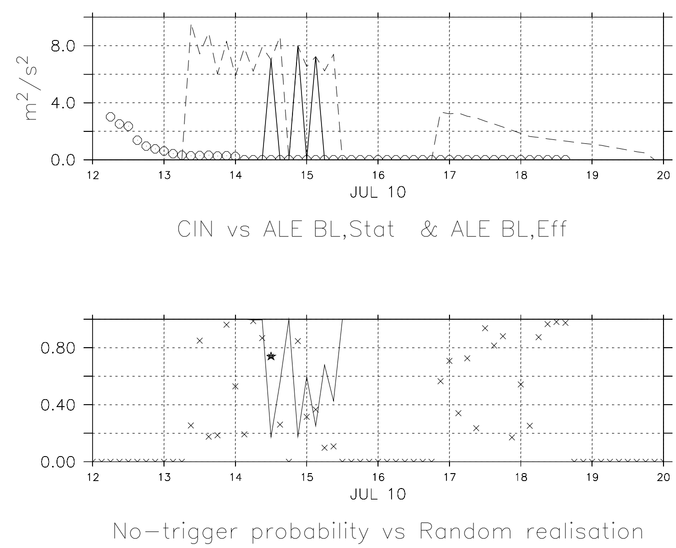

FIG. 6. AMMA Case: Time evolution of (a) |CIN| (J.kg^{-1}, circles), $\mathrm{ALE}_{\mathrm{BL,stat}}$ (m^2.s^{-2}, dashed) and $\mathrm{ALE}_{\mathrm{BL,eff}}$ (thick solid) and (b) Probability of no-trigger $\widehat{P}_{\Delta t}$ (solid), random sample $\mathcal{R}$ (crosses) and $\mathcal{R}$ at triggering (thick star) simulated by the SCM with deep convection switched off. The plume parameters are $\{a = 1 : b = 0.3 : \epsilon = 0.3 : \alpha = 0.33\}$ and the triggering parameters are $\{S_{\mathrm{trig}} = 12 : \tau = 600\}$

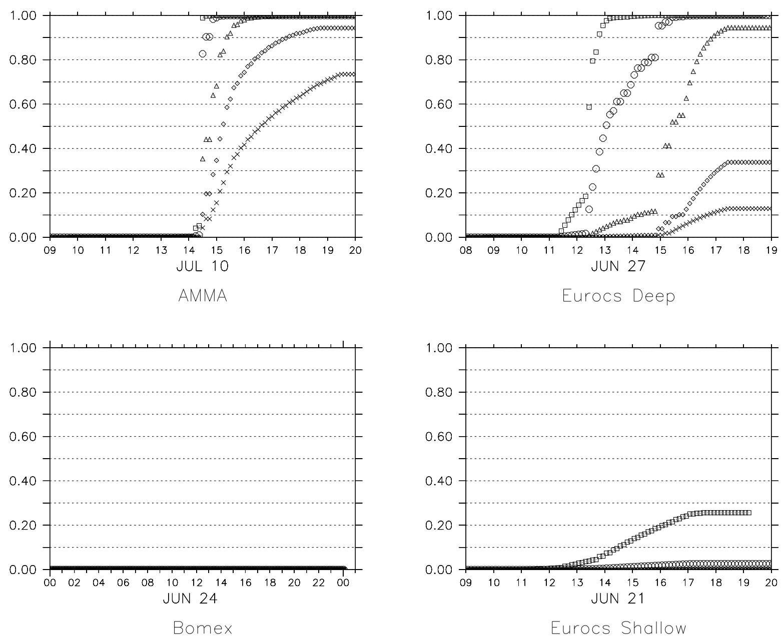

FIG. 7. Integrated trigger probability $\mathcal{P}_{\Delta t}$ for the threshold cross-sections $S_{\text{trig}} = 10$ km^2 (squares), 12 km^2 (circles), 15 km^2 (triangles), 18 km^2 (diamonds), 20 km^2 (crosses) for the case AMMA (upper left), EUROCS Deep (upper right), BOMEX (lower left) and EUROCS Shallow (lower right), with deep convection switched off. The plume parameters are $\{a = 1 : b = 0.3 : \epsilon = 0.3 : \alpha = 0.33\}$ and the triggering decorrelation time is $\tau = 600$ s.

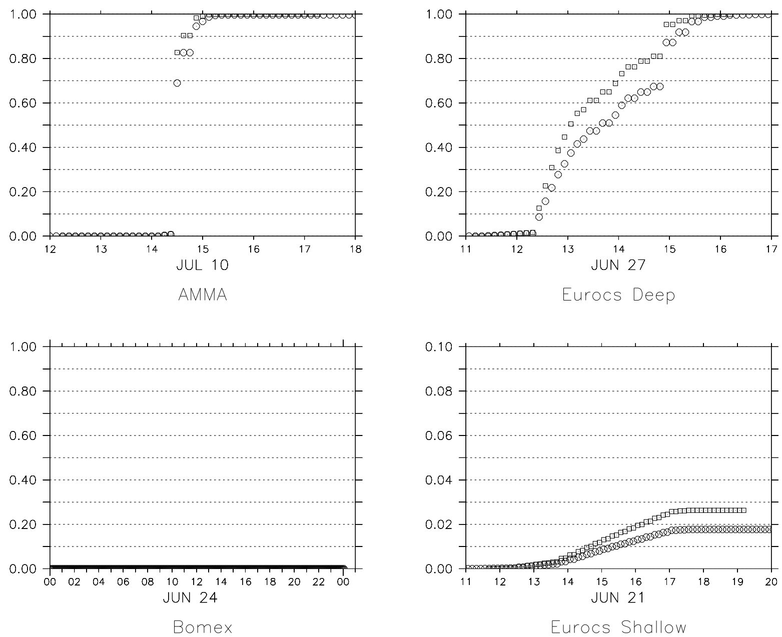

FIG. 8. Integrated trigger probability $\mathcal{P}_{\Delta t}$ for the decorrelation intervals $\tau = 600$ s (squares), 900 s (circles) for the case AMMA (upper left) and EUROCS Deep (upper right), BOMEX (lower left) and EUROCS Shallow (lower right) with deep convection switched off. The plume parameters are $\{a = 1 : b = 0.3 : \epsilon = 0.3 : \alpha = 0.33\}$ and the threshold cross-section is $S_{\rm trig} = 12$ km^2.

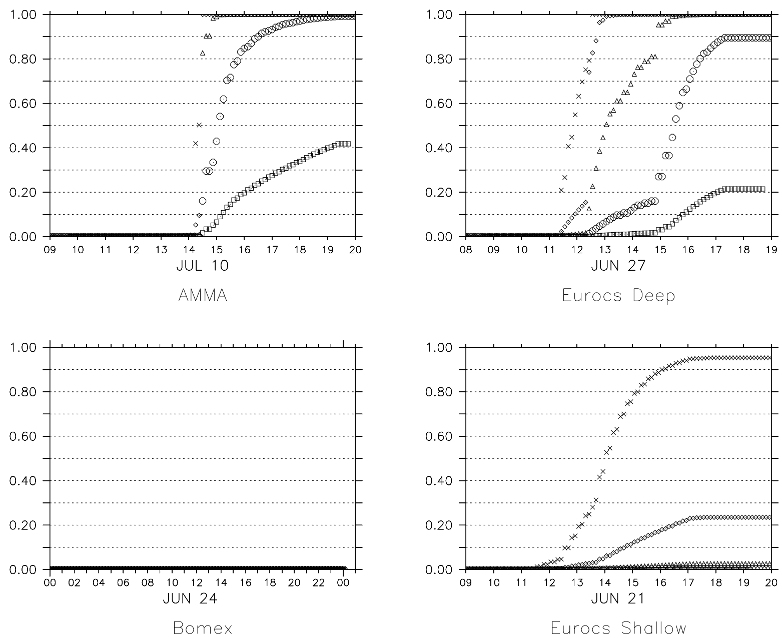

FIG. 9. Integrated trigger probability $\mathcal{P}_{\Delta t}$ for the domain area of reference $S_{\mathrm{d,Amma}} = 10^4$ km^2 (top left), $S_{\mathrm{d,Eu}} = 6,55.10^4$ km^2 (right), $S_{\mathrm{d,Bo}} = 2,5.10^5$ km^2 (lower left) multiplied by a factor $\beta = 0.01$ (squares), 0.1 (circles), 1 (triangles), 10 (diamonds), 100 (crosses) for the case AMMA (upper left), EUROCS Deep (upper right), BOMEX (lower left) and EUROCS Shallow (lower right), with deep convection switched off. The plume parameters are $\{a = 1 : b = 0.3 : \epsilon = 0.3 : \alpha = 0.33\}$ and the triggering parameters are $\{S_{\mathrm{trig}} = 12 : \tau = 600\}$.

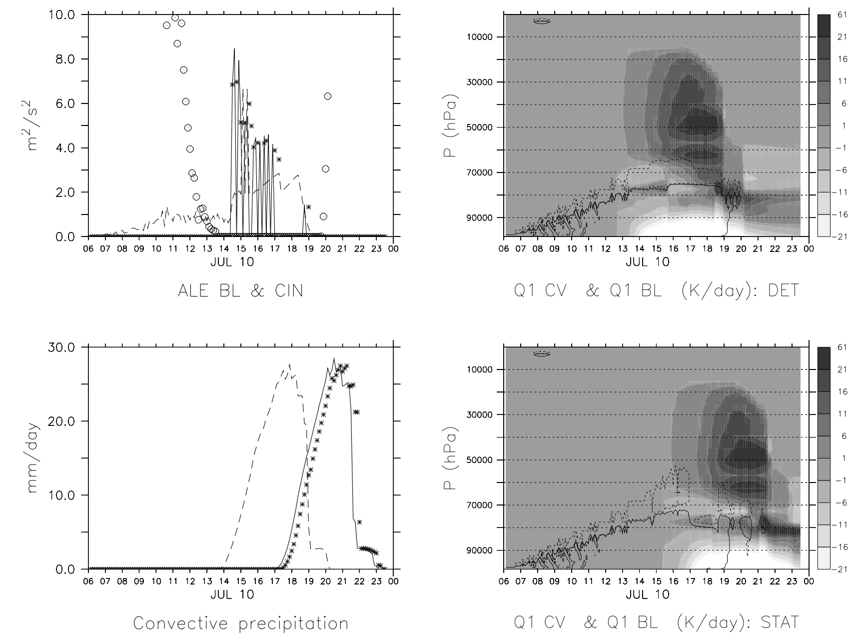

FIG. 10. AMMA Case: a) Upper-left panel: CIN (J.kg−1, circles) vs $\mathrm{ALE}_{\mathrm{BL}}$ ($\mathrm{m}^2.\mathrm{s}^{-2}$) for the deterministic run (dashed), the stochastic run 1 $\mathrm{ALE}_{\mathrm{BL,eff}}$ (solid) and the stochastic run 2 $\mathrm{ALE}_{\mathrm{BL,eff}}$ (crosses). b) Lower-left panel: Convective precipitation ($\mathrm{mm.hr}^{-1}$) for the deterministic run (dashed), the stochastic run 1 (solid) and the stochastic run 2 (crosses). c) Upper-right panel, Deterministic run: Deep convection heating rate ($\mathrm{K.day}^{-1}$) $Q_{1,\mathrm{CV}}$ (grey shaded), boundary layer processes heating rate ($\mathrm{K.day}^{-1}$) $Q_{1,\mathrm{BL}}$ (black contoured, thick lines for positive values and dashed lines for negative values). d) Lower-right panel, same for the Stochastic run 1. The plume parameters are $\{a = 1 : b = 0.3 : \epsilon = 0.3 : \alpha = 0.33\}$ and the triggering parameters are $\{S_{\mathrm{trig}} = 12 : \tau = 600\}$.

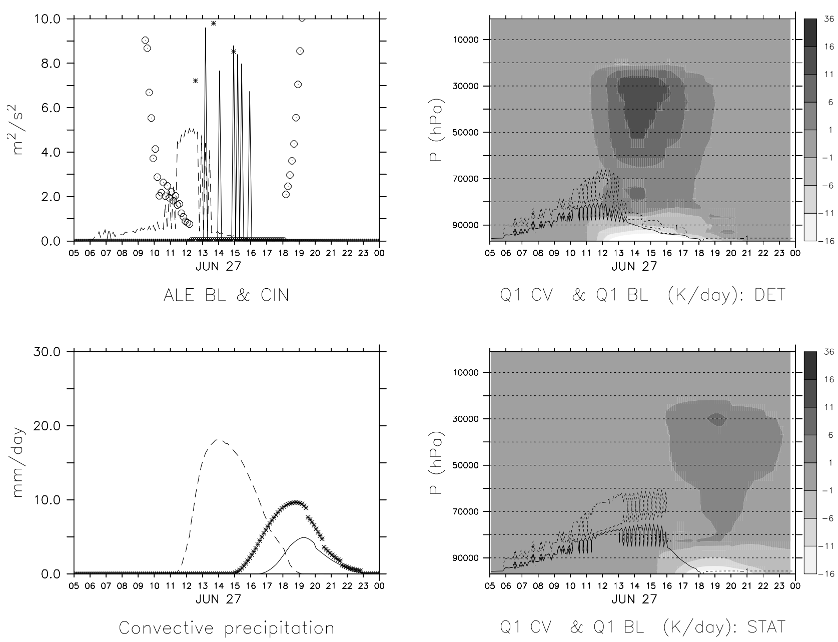

Fig. 11. EUROCS Deep Case: Same as Fig 10

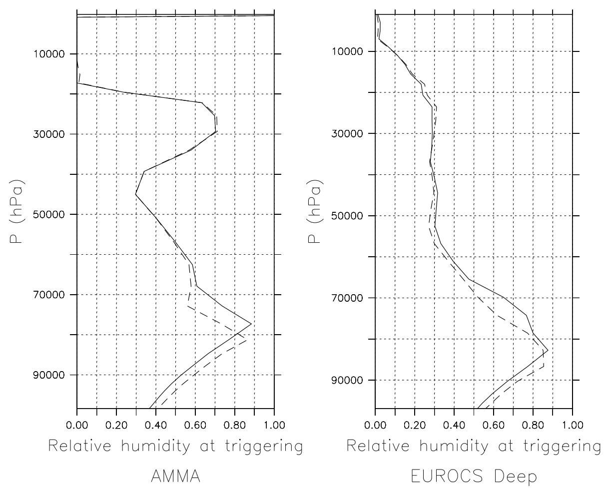

FIG. 12. Left panel, AMMA Case: Relative humidity profiles at triggering for the deterministic (dashed) and the stochastic (solid) runs given by the SCM. Right panel, same for the EUROCS Deep Case. The plume parameters are $\{a = 1 : b = 0.3 : \epsilon = 0.3 : \alpha = 0.33\}$ and the triggering parameters are $\{S_{\mathrm{trig}} = 12 : \tau = 600\}$.

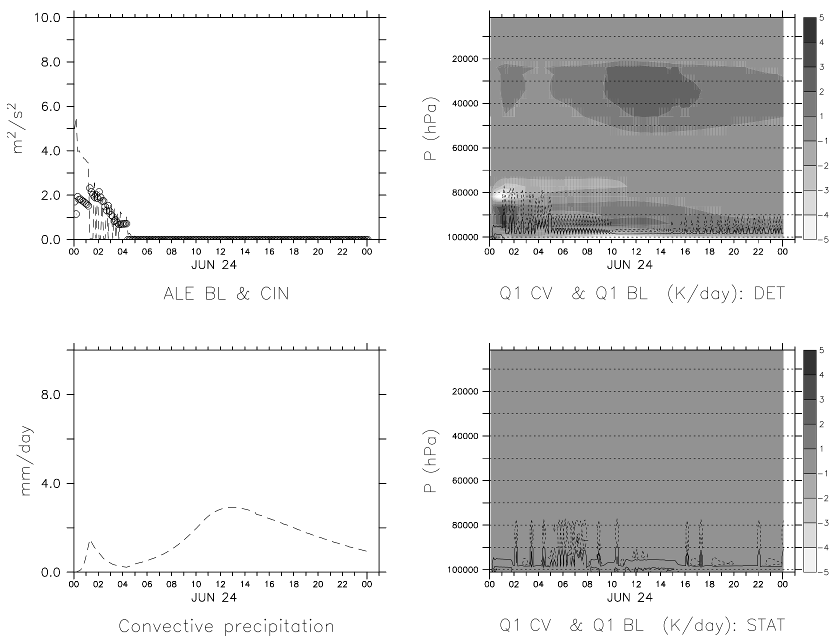

FIG. 13. BOMEX Case: a) Upper-left panel: CIN (J.kg−1, circles) vs Deterministic $\mathrm{ALE_{BL}}$ ($\mathrm{m^2.s^{-2}}$, dashed) and Stochastic $\mathrm{ALE_{BL,eff}}$ (solid), b) Lower-left panel: Convective precipitations($\mathrm{mm.hr^{-1}}$) for the deterministic (dashed) and the stochastic (solid) run, c) Upper-right panel, Deterministic run: Deep convection heating rate ($\mathrm{K.day^{-1}}$) $Q_{1,\mathrm{CV}}$ (grey shaded), boundary layer processes heating rate ($\mathrm{K.day^{-1}}$) $Q_{1,\mathrm{BL}}$ (black contoured, thick lines for positive values and dashed lines for negative values), d) Lower-right panel, same for the Stochastic run. The plume parameters are $\{a = 1 : b = 0.3 : \epsilon = 0.3 : \alpha = 0.33\}$ and the triggering parameters are $\{S_{\mathrm{trig}} = 12 : \tau = 600\}$.

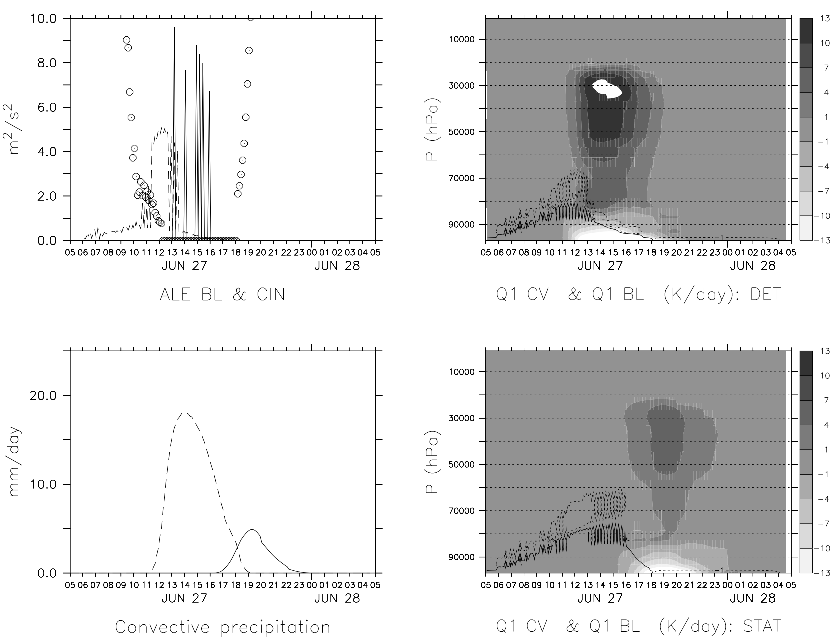

Fig. 14. EUROCS Shallow Case: Same as Fig 13

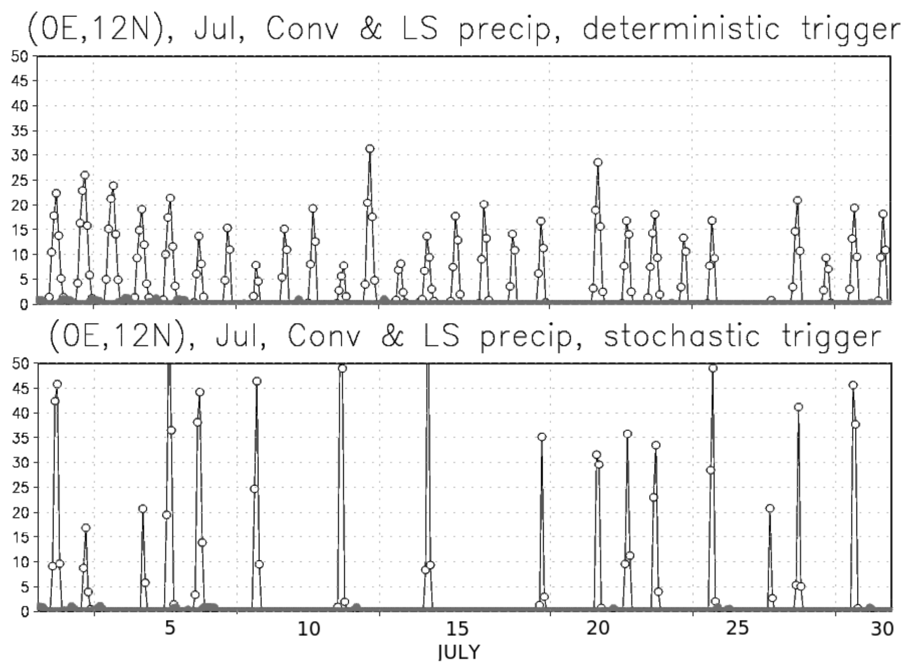

FIG. 15. Time series of convective (thin black) and large scale (thick grey) precipitation (mm.hr^{-1}) over Niamey (Niger) for the month of July, as simulated by LMDZ5. Upper panel: Deterministic case. Lower panel: Stochastic case. The plume parameters are $\{a = 1 : b = 0.3 : \epsilon = 0.3 : \alpha = 0.33\}$ and the triggering parameters are $\{S_{\rm trig} = 12 : \tau = 600\}$.